Impacts of Operators' Behavior on Reliability of Power Grids during Cascading Failures

Zhuoyao Wang, Mahshid Rahnamay-Naeini, *Member, IEEE,* Joana M. Abreu, Rezoan A. Shuvro, Pankaz Das, Andrea A. Mammoli, *Member, IEEE,* Nasir Ghani, *Senior Member, IEEE,* and Majeed M. Hayat, *Fellow, IEEE*

***Abstract*—Human operators play a key role in the reliable operation of critical infrastructures. However, human operators may take actions that are far from optimum. This can be due to various factors affecting the operators' performance in time-sensitive and critical situations such as reacting to contingencies with significant monetary and social impacts. In this paper, an analytic framework is proposed based on Markov chains for modeling the dynamics of cascading failures in power grids. The model captures the effects of operators' behavior quantified by the probability of human error under various circumstances. In particular, the observations from historical data and information obtained from interviews with power-system operators are utilized to develop the model as well as identify its parameters. In light of the proposed model, the non-critical regions of power-system's operating characteristics with human-factor considerations are characterized under which the probability of large cascading failures is minimized.**

***Index Terms*—Cascading failures, human factors, criticality, analytic model, blackout probability, power-grid operators, cyber-physical infrastructure**

I. Introduction

Critical infrastructures, such as power grids, are being increasingly equipped with advanced technologies and mechanisms including monitoring, automated control, intelligence and computational resources to enhance their reliability. However, human operators remain to be a key element in the reliable operation of such systems with often critical decisions to make and actions to take. In particular, the historical data of various infrastructure contingencies, such as the 2003 Northeast [1] and the 2011 Southwest [2] blackouts, show a clear track of operators' decisions and actions that significantly contributed, both positively and negatively, in the events. Specifically, critical and stressful situations, such as reacting to contingencies with significant monetary and social impacts, can affect human performance and increase the likelihood of human errors in decisions and actions. As discussed in [3], [4], it is not easy to model the human component in vulnerability analysis of critical infrastructures; however, efforts with various focuses on different infrastructures and contingency scenarios have emerged to address the critical need for understanding the role of human factors in the reliability of power-grid operations [5]–[9].

It is well known that large-scale blackouts in power grids are typically caused by cascading failures. The risk and high impact of cascading failures have attracted the attention of many researchers in the past and they have exerted considerable efforts in understanding and characterizing this phenomenon [10]–[18]. Nonetheless, the role of human factors in cascading failures has not been modeled and investigated analytically in the existing studies to the best of our knowledge.

Several factors can shape the performance of human operators in making critical decisions with potentially detrimental or beneficial effects on the physical system. Examples of such factors include the psychological state of the operators at the time of the event, level of stress, fatigue, level of experience, the amount of time to respond to a situation, knowledge and awareness about the situation, etc. Many of these factors are tied to the state of the physical system, and as the physical system evolves in time so do these factors and consequently the performance of human operators. At the same time, the human operators' performance can directly affect the state of the physical system through decisions and actions. As such, there is a coupling between the dynamics of the physical system and the human factors, which makes the analysis of cascading failures particularly challenging.

In this paper, we capture the coupling between the human factors and the power grid in an analytic framework. In particular, the proposed framework consists of two key components: (i) a Markov-chain model for the dynamics of cascading failures in the power grid, and (ii) a human reliability assessment model to characterize the probability of human error (by utilizing the Standardized Plant Analysis Risk-Human (SPAR-H) Reliability Analysis Method [19]) to investigate the effects of human factors on the progression of cascading failures in the power grid. These components are integrated together through various model parameters and state variables to capture the coupling between cascading dynamics and the human factors.

The proposed framework enables us to investigate the effects of human behavior on cascading phenomenon in power grids. We specifically characterize the probabilities of progression of cascading failures with various sizes of blackouts under various disturbance scenarios. We further provide the non-critical region of power-system operating characteristics

This work was supported by the DTRA's basic research program under grant No. HDTRA1-13-1-0020 and NSF's grant No. 2GA11 NSF CRISP.

Zhuoyao Wang (e-mail: wzy0791@gmail.com), Rezoan A. Shuvro, Pankaz Das and Majeed M. Hayat (e-mail: hayat@unm.edu) are with the Department of Electrical and Computer Engineering and Center for High Technology Materials, University of New Mexico, Albuquerque, NM 87131, USA.

Mahshid Rahnamay-Naeini (e-mail: mahshid.naeini@usf.edu) and Nasir Ghani are with Electrical Engineering Department, University of South Florida, Tampa, FL 33620, USA.

Joana M. Abreu is with the Fraunhofer Center for Sustainable Energy Systems (CSE), Boston, MA 02210, USA.

Andrea Mammoli is with Mechanical Engineering Department, University of New Mexico, Albuquerque, NM 87131, USA.

Zhuoyao Wang is presently with Tencent, Shenzhen, China.

(including loading level, load-shedding constraints and line-tripping threshold), which makes the power grid behave less vulnerable to cascading failures (i.e., the blackout size is distributed exponentially rather than one with a power-law tail), while considering the effects of human behavior.

II. Related Work

In this section we review three categories of work related to this paper. The first category is the work on the analysis of human reliability and performance. The second category of related work is on modeling the impact of human factors on critical infrastructures. The third and last category is on the modeling of cascading failures in power grids.

Human error can affect the system's performance just like any other technical flaw [20]. Human reliability analysis (HRA) is a technique designed to determine the critical aspects and the errors that can affect human decision making. HRA encapsulates the following steps: description of tasks in a chain of events, dependence among tasks, procedures and processes, situation awareness and cognitive conditions of the decision maker [5]. The SPAR-H is a simplified approach to human-error quantification that accounts for individual perception processing and response to events in complex environments [21]. The method relies on the multiplicative effect of performance shaping factors (PSFs), which are variables that describe the situation or the psychological condition of the human operators. Each factor contains levels of severity. The outcome of the SPAR-H methodology is the calculation of a total Human Error Probability (HEP) for every diagnosis or action in the event tree [22]. Abreu *et al.* [7] modeled the HEP in various failure scenarios by interviewing power-system operators with different levels of expertise. In [8], Panteli and Kirschen investigated how insufficient operators' situation awareness affect cascading failures in power systems; then a generic procedure was presented for achieving sufficient situation awareness.

As for the second category of the related work, we review the existing models that investigated the impact of human factors in critical infrastructures. In [13], Anghel *et al.* presented a stochastic model to provide a comprehensive representation of the complex behavior of both the grid dynamics under random perturbations and the operator's response to the contingency events. This model described the utility response to various disturbances in an attempt to include a description of the human response to contingency events. Numerical results were presented to cast the optimization of operators' response into the choice of the optimal strategy for mitigating the impact of random component failure events and, possibly, for controlling blackouts. In [6], Lawton and Gauthier developed an approach to integrate human performance modeling into a large scale system-of-systems (SoS) simulation toolset. The SoS-scale analysis on human performance was presented and the utility of the toolset was illustrated by an example problem. In [9], Bessani *et al.* introduced a stochastic model to enable the incorporation of human operators' performance in a sequential Monte-Carlo simulation that integrates the response time in reliability of power systems. Their results showed that the response time of the operators affects the reliability that are related to the durations of the failure, indicating that a fast decision directly contributes to the system performance. In [23], Moura *et al.* introduced the multi-attribute technological accidents dataset (MATA-D) containing detailed investigation reports from the past major accidents and used it to address the manifestation of human errors.

As for the third category of related work, we shall discuss the probabilistic models and statistical analysis of cascading failures in power grids. In [24], Carreras *et al.* asserted that the frequency distribution of the blackout sizes does not decrease exponentially with the size of the blackout, but rather has a power-law tail. Such important observation was obtained from the analysis of a 15-year time series of blackouts in the North American electric power transmission system. A simplified power-transmission-system model was then presented to examine the criticality of cascading failures in the transmission system. The model considered the DC power flow approximation and standard linear programming optimization of the generation dispatch. In [25], Kirschen *et al.* proposed a technique to calculate a probabilistic indicator of the stress (i.e., criticality) in a power system. This technique was based on the establishment of a calibrated scale of reference cases and on the use of correlated sampling in a Monte-Carlo simulation. In [12], Dobson *et al.* proposed an analytically tractable model, termed CASCADE, to study the load-dependent cascading failures. The results obtained from the CASCADE model showed that the saturating quasibinomial distribution of the number of failed components had a power-law region at a critical loading and a significant probability of total failure at higher loading. As an aggregation of the above works, Nedic *et al.* [26] further verified and examined the criticality in a 1000-bus network with an AC power flow model that represents many of the interactions that occur in cascading failures. It was found that at the critical loading there was a sharp rise in the mean blackout size. A power-law probability distribution of blackout size was also observed, which indicates a significant risk of large blackouts. In [27], Rahnamay-Naeini and Hayat conducted sensitivity analysis of power grids to cascading failures and showed the critical dependence of cascading failures (i.e., blackout-size distributions with power-law tails) on the operating characteristics, including the loading level, load-shedding constraints and the line-tripping threshold.

III. Impact of Human Factors on Cascading Failures

Generally, large-scale blackouts result from the cascading effect of component failures triggered by initial disturbances such as hurricanes, earthquakes, operational faults, sabotage occurrences, and physical attacks such as weapons of mass destruction. The term cascading failures refers to the successive inter-dependent outages of the components of an electric-power system in a short duration of time due to a combination of initial failures and lack of timely corrective actions. It has been known that the number of successive failures when cascading failures occur increases exponentially in time [28], which may prevent the implementation of corrective actions in a timely fashion.

For a better illustration of how human factors (e.g., operators' response to events, power-system control/monitor software, etc.) can impact cascading failures, we provide two narratives extracted from historical data as the evidence. The first narrative is the 2003 Northeast blackout, which is summarized from the blackout reports [1]. Our second narrative is about the 2011 Southwest blackout, which is caused by a network operator's error in the power-distribution layer.

The 2003 Northeast Blackout: The Northeast blackout of 2003 was a widespread power outage that occurred throughout parts of the Northeastern and Midwestern United States and the Canadian province of Ontario on Thursday, August 14, 2003. The outage affected more than 50 million people.

The event started from the mistake by a control room operator, who forgot to restart the inoperative power flow monitoring tool at 12:15 pm after he corrected the telemetry problem of the state estimator. At 1:31 pm, the Eastlake generating plant, owned by FirstEnergy (FE), shut down. At 2:02 pm, the first of several 345-kV overhead transmission lines in northeast Ohio failed due to contact with a tree. In the meantime, an alarm system failed at FE's control room and was not repaired. As a result, control room operators were not able to recognize or understand the deteriorating condition of the power grid in time. To make matters worse, the lack of alarms affected control room operators' judgment and misled them. For example, the control room operators took no action later to the voltage dips in the grid, failed to inform system controllers, and even dismissed a call from American Electric Power about the tripping of a 345-kV shared transmission line in northeast Ohio. Due to the various human-related errors described above, there was no correct response to the initial few contingencies that occurred in the power grid. As a result, a large cascading failure occurred after 3 pm and progressed rapidly. By 4 pm, five 345-kV transmission lines and sixteen 138-kV transmission lines were tripped offline due to overload (e.g., under voltage and over current).

After 4:05 pm, the cascading failure accelerated and spread to the whole northeastern grid within five minutes, in which more transmission lines were tripped. At this time, operators in different areas realized the blackout and executed grid separations to divide the whole northeastern grid into isolated sub-grids for protection. Finally at 4:13 pm, the outage ended with 256 power plants off-line, where 85% of the power plants went offline after the grid separations occurred, most due to the action of automatic protective controls. The 2003 Northeast blackout clearly indicated that human error can be the cause of severe cascading failures.

The 2011 Arizona–Southern-California Outages: On the afternoon of September 8, 2011, an 11-minute system disturbance occurred in the Pacific Southwest, leading to cascading outages and leaving approximately 7 million people without power.

A single 500-kV transmission line initiated the event, but it was not the sole cause; the system was designed to operate in an N-1 state. In this situation, the redistribution of this line's power created voltage deviations and overloads, which had a ripple effect as transformers, transmission lines, and generating units tripped offline. During the 11 minutes of the event, the Western Electricity Coordinating Council (WECC) reliability coordinator issued no directives and only limited mitigating actions were taken by the transmission operators of the affected areas. As a result of the cascading outages stemming from this event, customers in the SDG&E, IID, APS, western area power administration-lower Colorado, and CFE territories lost power, some for multiple hours extending into the next day. It took almost 12 hours for all the affected entities to restore power. Analysis of this blackout showed that the system was not being operated in a secure N-1 state. This failure stemmed primarily from weaknesses in two broad areas: operations planning and real-time situational awareness. If these were done properly it would have allowed system operators to proactively operate the system in a secure N-1 state during normal system conditions and to restore the system to a secure N-1 state as soon as possible, but no longer than 30 minutes. Without adequate planning and situational awareness, entities responsible for operating and overseeing the transmission system could not ensure reliable operations within system operating limits or prevent cascading outages in the event of a single contingency.

It is clear from the two narratives that human factors can highly influence the cascading failure in power grids. Next, we proceed to utilize the SPAR-H methodology to estimate the HEP for the human failure events in probabilistic risk assessment. HEP is the conditional probability of human error given the performance context. The context is represented by a set of variables, the PSFs, which is shown in Table I. Each variable plays a role in the way that the operators respond to an unpredictable event. The final probability of error can be calculated by the following formulas [7]:
a) for number of PSFs < 3

$$\text{HEP} = \text{NHEP} \cdot \prod_{i=1}^{2} \text{PSF}_i, \tag{1}$$

b) and for number of PSFs ≥ 3

$$\text{HEP} = \frac{\text{NHEP} \cdot \prod_{i=1}^{8} \text{PSF}_i}{\text{NHEP} \cdot \prod_{i=1}^{8} \text{PSF}_i + 1}. \tag{2}$$

The term NHEP is short for nominal human error probability, which is dependent on whether the current scenario is diagnosis (0.01) or action (0.001). It is worth noting that there could be more than one power-system operator handling the failure events occurred during cascading failures. For simplicity, the associated multiplier of the PSFs in Table I are assumed to represent the aggregate effect of multiple operators when calculating the HEP.

To this end, the probability of human error in any scenario (e.g., during cascading failures) can be quantified. This will, in turn, be utilized in developing our analytic probabilistic cascading-failure model proposed in the next section.

IV. Analytic Framework

A. Three Phases of Cascading Failures

Observed from historical blackout data (e.g., the two narratives given in Section III), a cascading failure can be typically divided into three phases: the *precursor phase* (phase-1), the *escalation phase* (phase-2) and the *fade-away phase* (phase-3).

TABLE I
PERFORMANCE-SHAPING FACTORS AND THEIR MULTIPLIERS (TABLE IS ADOPTED FROM [19]. THE TERM "PF" STANDS FOR PROBABILITY OF FAILURE.)

SPAR-H PSFs	SPAR-H PSF levels	Multiplier
NHEP: Diagnosis / Action		0.01 / 0.001
Available time	Inadequate time	Pf = 1
	Minimum required time	10
	Nominal time	1
	Extra time	0.1
	Expansive time	0.01
Stress/Stressors	Extreme	5
	High	2
	Nominal	1
Complexity	Highly complex	5
	Moderately complex	2
	Nominal	1
	Obvious diagnosis	0.1
Experience/training	Low	10
	Nominal	1
	High	0.5
Procedures	Not available	50
	Incomplete	20
	Available, but poor	5
	Nominal	1
	Diagnostic	0.5
Ergonomics/HMI	Missing / misleading	50
	Poor	10
	Nominal	1
	Good	0.5
Fitness for duty	Unfit	Pf = 1
	Degraded fitness	5
	Nominal	1
Work processes	Poor	2
	Nominal	1
	Good	0.8

In the beginning of a cascading failure, there is a small number of initial and subsequent events such as transmission-line failures in the power grid. This stage is termed the precursor phase. As the cascading failure spreads in the power grid, the number of transmission-line failures increases rapidly, which gives rise to the escalation phase. When a large number of transmission lines have failed, the power grid is divided into islands and the cascading failure starts to phase out. This stage is termed the fade-away phase.

For ease of understanding, we show the time evolution of the cascading failure in the 2003 Northeast US blackout as well as the associated three cascading phases in Fig. 1.

B. The hSASE Cascading-Failure Model

Developing an analytic model for cascading failures in the power grid is highly challenging. This is due to the fact that there is a large number of physical attributes of the power grid such as power generation, substation loads, power-flow distribution through transmission lines, functionality of components, voltage and phase of transmission lines and buses, etc., which collectively contribute to a cascading failure. Therefore, keeping track of all the details in the analytic model will result in severe scalability issues.

To address such scalability challenge, we have previously developed a methodology [15], termed abstract state space. To describe it briefly, the space of all detailed power-grid states

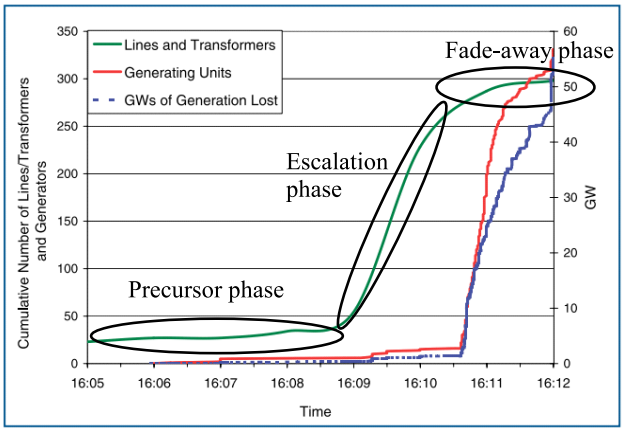

Fig. 1. Time evolution and the associated three phases of the cascading failure in 2003 Northeast US blackout. (Figure is adopted from [28].)

is partitioned into a collection of equivalence classes. The detailed power-grid states in the same class are represented by the Cartesian product of a few aggregate state-variables with the same values. Such coarse partitioning of the state space of the power grid implies that detailed power-grid states in the same class will be indistinguishable as far as the reduced abstraction is concerned. To this end, each class of the power-grid states is termed an abstract state.

In this paper, we further extend the abstract state space and use three state variables to represent an abstract state of the power grid with the consideration of operator's response (OR). More precisely, a 3-tuple (F_i, H_i, I_i) is used to represent an abstract state (or in short a state) S_i of the power grid during a cascading failure (i.e., $S_i = (F_i, H_i, I_i)$): the state variable F_i denotes the failed number of transmission lines, and the state variable H_i, termed the level of OR, specifies the status of human operators facing power-system situation at state S_i.

As in [15], we term the state S_i with $I_i = 0$ and $I_i = 1$ as *transitory* and *absorbing* states, respectively. If the power grid is in a transitory state, then the cascading failure will keep proceeding. On the other hand, the cascading failure terminates if the power grid is currently in an absorbing state. Furthermore, we assume that the transition probability from a state S_i to other states is fully determined by S_i (or specifically F_i, H_i and I_i). Hence, a cascading-failure process in a power grid can be modeled as a Markov chain. The analytic model presented in this paper is then termed the human-factor-coupled stochastic abstract-state evolution (hSASE) model, which is a generalization to the SASE model developed in [15].

Similarly to most of the existing cascading-failure models, transmission-line restoration is not considered in the hSASE model. This is due to the fact that power-system operators typically would not restore the failed (or tripped) transmission lines during cascading-failure events. Furthermore, as in [15], we assume that time is divided into small time slots such that only one failure can occur in each time slot. To this end, two types of state transitions, which are triggered by transmission-line failures, will be considered. The first type is called *cascade-stop* transition, where a transitory state S_i

TABLE II
FOUR OPERATORS' RESPONSE LEVELS AND THE ASSOCIATED TWO PSFS DURING A CASCADING FAILURE IN IEEE 118-BUS SYSTEM

Operators' Response	Definition	Available time (respond to contingencies)	Stress (of operators)
Level 1	$F \leq 5$ and $C^{\max} \leq$ 80MW	Extra time	Nominal
Level 2	$5 < F \leq 10$ or 80MW $< C^{\max} <$ 500MW	Nominal time	High
Level 3	$10 < F \leq 50$ or $C^{\max} \geq$ 500MW	Minimum required time	Extreme
Level 4	$F > 50$	Inadequate time	N/A

transitions to an absorbing state S_j such that $F_j = F_i$ and $H_j = H_i$. Note that there will be no more transitions if the system enters an absorbing state. The cascade-stop transition leads to an end of a cascading-failure process. The second type of transitions is a *cascade-continue* transition, where a transitory state S_i transitions to another transitory state S_j with the proviso that $F_j = F_i + 1$ and $H_j \geq H_i$. Now the new transitory state S_j may transition to an absorbing state or to another transitory state, and so on. Note that the cascade-continue transitions are assumed to be caused by single failures; hence, S_j always has one more failure than the preceding transitory state S_i, i.e., $F_j = F_i + 1$. It is also natural to assume that a state S_i with $F_i = L$, where L is the total number of transmission lines in the power grid, is an absorbing state. The cascade-stop and cascade-continue transitions considered in the hSASE model are similar to those in the SASE model [15]; however, the impacts of human error on cascading failures are not considered in the SASE model, i.e., operators are assumed to respond perfectly to any contingency occurred in the power grid.

As the cascade progresses and failures accumulate in the power grid, the level of OR also changes. The coupling between the level of OR and state of the power grid can be explained as follows. Initially when cascading failures start in the power grid, the level of OR reflects less stress and more time for the operators to react to the situation. However, as the failures accumulate (especially the failures of critical transmission lines with large power-flow capacities), the state of the power grid will impose a higher stress and less time to react. Finally, when the cascade starts to phase out the level of OR will reflect less stress (as the event has already happened) and more time to react. As discussed above, the state of the power grid specifies the level of OR. On the other hand, the level of OR specifies the performance of human operators, which will affect the state of the power grid. Specifically in the first two cascading phases the impact of the operators' performance on cascading failure will be more significant compared to the third (namely the last) cascading phase.

In the remainder of this subsection, we use the IEEE 118-bus system as an example to illustrate the connection between the levels of OR and the three phases of cascading failures. In the IEEE 118-bus system, there are 186 transmission lines in total. We further assume that there are five possible power-flow capacities (e.g., 20MW, 80MW, 200MW, 500MW and 800MW representing the quantized power flow capacities based on line properties) associated with the 186 transmission lines. It is noted that these specific capacity values are estimated, since the necessary information for determining the capacities of transmission lines, such as physical properties of the line (e.g., length) and thermal characteristics, are not available publicly. To choose the five capacity values, we have calculated the power flow through the lines using the default setting under normal operating condition given by MATPOWER [29]. After identifying the power flows under the default setting, we quantized them into five capacity classes to ensure the tractability of the analytic framework while keeping the size of the state space to a minimum.

Now let H be the set containing all the levels of OR in the hSASE model. We assume four levels of OR to capture the state of human operators' performance factors during cascading failures in the IEEE 118-bus system. In brief, a higher level of OR implies a higher risk for any of the PSFs (e.g., the available time for power-system operators to respond to contingencies becomes inadequate and stress of operators increases as the level of OR goes up). For simplicity, in this preliminary study we only consider two important PSFs listed in Table I: the available time for operators to respond to contingencies and the stress of operators.

For the ease of understanding, the four levels of OR are further described next in more detail. We use F and $C^{\max}$ to represent the number of failed transmission lines and the maximum (power-flow) capacity of the failed lines in the corresponding levels.

Level 1: When $F \leq 5$ and $C^{\max} \leq$ 80MW, we say that the OR is at level 1. In this stage, the power grid is in the precursor phase and there are a few initial failures. The operators have more than adequate time to respond to the contingencies (e.g., between 1 and 2 times the nominal time) and operators' stress is nominal. Accordingly, the PSFs 'Available time' and 'Stress' are with levels 'Extra/Expansive time' and 'Nominal,' respectively, as shown in Table I.

Level 2: When $5 < F \leq 10$ or 80MW $< C^{\max} <$ 500MW, we say that the OR is at level 2. In this stage, the power grid is in the advanced precursor cascading phase and additional failures have occurred, either due to the propagation of the initial failures or due to a large initial impact from physical attacks such as deliberate attacks or natural disasters. The operator knows that there is a risk for a cascading failure due to the disaster caused by large initial failures; however, there is still sufficient time to respond to the contingencies yet the stress at this stage is higher than that for Level 1. Accordingly, the PSFs 'Available time' and 'Stress' are with levels 'Nominal time' and 'Nominal,' respectively, as shown in Table I.

Level 3: When $10 < F \leq 50$ or $C^{\max} \geq$ 500MW, we say that the OR is at level 3. At this stage, cascading failures are progressing rapidly in the power grid. The available time for operators to respond to contingencies is the minimum required time; thus, the operators' stress is extremely high.

Accordingly, the PSFs 'Available time' and 'Stress' are with levels 'Minimum required time' and 'Extreme,' respectively, as shown in Table I.

Level 4: We declare this level when $F > 50$ in the IEEE 118-bus system. At this stage, cascading failures phase out in the power grid and operators' performance cannot alter the state of failures since a large blackouts has already occurred. Hence, the PSF 'Available time' is at the level of 'Inadequate time' as shown in Table I and there is no need to take the operators' stress into account.

For convenience, we have listed the definitions of the four OR levels in Table II. It is worth noting that the level of OR associated to a state S_i (namely H_i) is determined by F_i and $C_i^{\max}$, where $C_i^{\max}$ is the maximum capacity of failed transmission lines at S_i. This implies that a state S_i in the hSASE model is implicitly determined by F_i, I_i and $C_i^{\max}$. Hence, the transition of states is achieved by tracking the accumulation of the failed transmission lines as well as the increment of the maximum capacity of the failed transmission lines in the power grid. The detailed modeling of transition probabilities is provided in the next subsection.

C. Transition Probabilities in the Markov Chain

In this section, we model the transition probabilities from a state S_i to other states S_j. It is trivial that if S_i is an absorbing state, then

$$P(S_j|S_i) = \begin{cases} 1 & \text{if } i = j, \\ 0 & \text{if } i \neq j. \end{cases} \tag{3}$$

For a transitory state S_i, the transition probabilities $P(S_j|S_i)$ are summarized as follows.

For $F_i \leq 10$, $S_i \neq (5,1,0)$ and $S_i \neq (10,2,0)$,

$$P(S_j|S_i)=\begin{cases} \text{(i) } P_{\text{stop}}(F_i)g(H_i) & \text{if } I_j = 1, \\ \text{(ii) } 0 & \text{if } I_j = 0 \text{ and } H_j < H_i, \\ \text{(iii) } \big(1-P_{\text{stop}}(F_i)g(H_i)\big)\frac{\sum_{C_i=1}^{H_i} L_{C_i}-F_i}{L-F_i} & \text{if } I_j = 0 \text{ and } H_j = H_i, \\ \text{(iv) } \big(1-P_{\text{stop}}(F_i)g(H_i)\big)\frac{L_{C_j}}{L-F_i} & \text{if } I_j = 0 \text{ and } H_i < H_j \leq 3. \end{cases} \tag{4}$$

When $S_i = (5,1,0)$,

$$P(S_j|S_i)=\begin{cases} \text{(i) } P_{\text{stop}}(F_i)g(H_i) & \text{if } I_j = 1, \\ \text{(ii) } 0 & \text{if } I_j = 0 \text{ and } H_j \leq H_i = 1, \\ \text{(v) } \big(1-P_{\text{stop}}(F_i)g(H_i)\big)\frac{\sum_{C_i=1}^{H_j} L_{C_i}-F_i}{L-F_i} & \text{if } I_j = 0 \text{ and } H_j = H_i + 1 = 2, \\ \text{(iv) } \big(1-P_{\text{stop}}(F_i)g(H_i)\big)\frac{L_{C_j}}{L-F_i} & \text{if } I_j = 0 \text{ and } H_i + 1 < H_j \leq 3. \end{cases} \tag{5}$$

When $S_i = (10,2,0)$,

$$P(S_j|S_i)=\begin{cases} \text{(i) } P_{\text{stop}}(F_i)g(H_i) & \text{if } I_j = 1, \\ \text{(ii) } 0 & \text{if } I_j = 0 \text{ and } H_j \leq H_i = 2, \\ \text{(v) } \big(1-P_{\text{stop}}(F_i)g(H_i)\big)\frac{\sum_{C_i=1}^{H_j} L_{C_i}-F_i}{L-F_i} & \text{if } I_j = 0 \text{ and } H_j = H_i + 1 = 3. \end{cases} \tag{6}$$

and when $F_i > 10$,

$$P(S_j|S_i) = \begin{cases} \text{(i) } P_{\text{stop}}(F_i)g(H_i) & \text{if } I_j = 1, \\ \text{(vi) } 1 - P_{\text{stop}}(F_i)g(H_i) & \text{if } I_j = 0. \end{cases} \tag{7}$$

We have considered four scenarios (or groups of states) in the power grid represented by (4)-(7). All the possible state transitions are further categorized into six cases (labeled by cases (i), (ii), (iii), (iv), (v) and (vi), respectively), where the expression of the transition probability for each case is the same for all the scenarios. Note that (5), (6) and (7) represent the transition probabilities for a specific S_i, while (4) is the general expression used for the rest of the S_i. Detailed explanation of the six cases of transitions are given below.

- Case (i) represents a transition from a transitory state S_i to an absorbing state S_j. The term $P_{\text{stop}}(F_i)$ is the cascade-stop probability obtained based on the power-system simulations. We emphasize here that such cascade-stop probability is obtained without the consideration of human error in the simulator. More specifically, we assume that the operators are always performing the correct response to the contingencies. The function g captures the impact of operators' performance, namely human error, on the cascading failure. The range of the function g is $[0,1]$. Since we utilize two PSFs in the model, the HEP of a state S_i is then calculated by (1) as discussed in Section III. It is noted that as HEP increases, the function g reduces the probability of transiting to an absorbing state. The detailed definition and characterization of function g is presented in Section IV-D.
- Case (ii) represents the transition from a transitory state S_i to a transitory state S_j with H_j less than H_i. The transition probability equals zero for cases (ii), because these transitions cannot occur. More specifically, the maximum capacity of failed transmission lines cannot decrease during a cascading failure.
- Cases (iii) and (iv) represent the general cascade-continue transitions from a transitory state S_i to another transitory state S_j. Here L_{C_i} is the number of transmission lines whose capacity are specified by the ith level of OR. For example in the IEEE 118-bus system, L_{C_1} is the number of transmission lines that have capacity less than or equal to 80MW (namely OR = 1); L_{C_2} is the number of transmission lines that have capacity larger than 80MW but less than 500MW (namely OR = 2); and L_{C_3} is the number of transmission lines that have capacity larger than or equal to 500MW (namely OR = 3). Note that $L = \sum_{C_i=1}^{3} L_{C_i} = 186$ is total number of transmission lines in the power grid. The two transition probabilities for cases (iii) and (iv) are formulated based on an assumption that the next transmission line to be failed during the cascading failure is randomly selected from the rest of the functional transmission lines in the power grid. It is worth noting that H_i and H_j are less than or equal to three in cases (iii) and (iv) for the example studied here.
- Case (v) represents the same transition as case (iii); however, there is one more transmission-line failure whose capacity is less than or equal to the values specified by the ith level of OR. According to the definitions of the OR levels regarding F, however, when $S_i = (5,1,0)$ and $S_i = (10,2,0)$ such a transition will cause a rise in the level of OR (i.e., H_j =

H_i+1) while $H_j = H_i$ in case (iii). Note that the difference between the expressions in (iii) and (v) is the upper limit of the summation, i.e., H_i in case (iii) and H_j in case (v).

- Case (vi) represents the cascade-continue transitions for states S_i with $F_i > 10$. From Table II, it is noted that the level of OR of the state S_i with $F_i > 10$ is either at 3 or 4. In this case, the rise of the level of OR from 3 to 4 only depends on the number of failures (i.e., from $F_i = 50$ to $F_j = 51$), and the level of OR stays at 4 (namely the highest level) for states S_i with $F_i > 50$. Hence, the probability of transition from S_i with $F_i > 10$ to S_j with one more failure is always equals to one minus the probability that the cascading failure terminates at S_i, i.e., $P_{\text{stop}}(F_i)g(H_i)$.

D. Impact of Human Error on the Progression of Cascading Failures

In this section, we characterize the function g introduced in the transition probabilities in the previous subsection. The function g allows us to capture the impact of operators' response on the progression of cascading failures. This step will allow us to close the loop between the human factors and the dynamics of cascading failures in the power grid.

Naturally, as the HEP increases the probability of further failures in the system also increases because of erroneous decisions and actions. This implies that the probability of termination of the cascading failure decreases as the likelihood of human error increases. To capture these effects, we define

$$g(H_i) = 1 - b\text{HEP}(H_i) \tag{8}$$

to multiplicatively adjust $P_{\text{stop}}(F_i)$ based on the HEP. In this formulation, b is the free parameter for adjusting the strength of the human-error impacts. In particular, $g(H_i)$ will be multiplied by $P_{\text{stop}}(F_i)$ to determine the probability that the cascading failure terminates at state S_i (i.e., the term $P_{\text{stop}}(F_i)g(H_i)$ in (4)-(7)). Since $g(H_i)$ has a value in $[0, 1]$, it will reduce $P_{\text{stop}}(F_i)$.

In (8), if b is a constant (independent of H_i) then it is implied that the strength of the human-error impacts on failures does not directly depend on the phases of the cascading failure. However, the human error and decisions can have various degrees of impacts on the progression of failures depending on the state of the power system. For instance, the impact of erroneous decisions and actions by the operators are particularly severe on the likelihood of further failures during the precursor phase. As such, we consider larger values of b for this phase. On the other hand, we consider smaller values for b when cascading failures have already occurred and blackouts have affected large areas. This is because the role of human errors on further possible failures are less significant. In the final stage of cascading failures, we consider $b = 0$ (i.e., $g(H_i) = 1$) since operators' performance cannot alter the state of cascading failures in this stage as discussed earlier. In general, in this formulation the larger values of b represent more severe impacts of human errors on cascading failures. Specifically, based on these assumptions we consider b values as 10, 2.5, 1.5 and 0 for the four levels of OR, respectively.

E. Modeling P_{stop} using Three Operating Characteristics

As discussed in the previous sections, $P_{\text{stop}}(F_i)$ is one of the key elements of the transition probabilities in the hSASE model, which also needs to be characterized. In our earlier work [15], we have conducted extensive power-system cascading-failure simulations based on MATPOWER for investigating the behavior of $P_{\text{stop}}(F_i)$. In particular, we have observed from cascading-failure simulation results that $P_{\text{stop}}(F_i)$ is strongly affected by the following three intrinsic power-grid operating characteristics.

1) Power-grid loading level: We denote the power-grid loading level by r, defined as the ratio of the total demand to the generation-capacity of the power grid. The parameter r represents the level of stress over the grid in terms of the loading level of its components.

2) Line tripping threshold: We consider a threshold, α_k, for the power flow through the kth line above which the protection relay trips the line. Various factors and mechanisms in the power grid may affect the threshold α_k for transmission lines. These include, for example, the environmental conditions, failures in adjacent lines, and smaller measured impedance than relay settings due to overload [30]. We represent the difference between the nominal capacity of a line C_k^{opt} and α_k by a parameter e as $C_k^{\text{opt}} - \alpha_k = eC_k^{\text{opt}}$. The parameter e captures the effects of various factors and mechanisms that may lead to failure of transmission lines when their power flow is within a certain range of the maximum (nominal) capacity.

3) Load-shedding constraint level: Constraints in implementing load shedding are generally governed by control and marketing policies, regulations, physical constraints and communication limitations. The ratio of the uncontrollable loads (loads that do not participate in load shedding) to the total load in the power grid is termed the load-shedding constraint, denoted by θ. In extreme cases, $\theta = 1$ means load shedding cannot be implemented, and $\theta = 0$ means there is no constraint in implementing the load shedding.

The theoretical ranges of all the three operating characteristics can be from zero to one, i.e., r, e, $\theta \in [0, 1]$. As the value of any of the three operating characteristics increases, the power grid becomes more vulnerable to cascading failures. Figure 2 shows the simulation results of $P_{\text{stop}}(F_i)$ for the IEEE 118-bus system, which depicts the dependency of cascade-stop probability on F_i and the load-shedding constraint level of the power grid, θ. Following our earlier work [27], the formula of $P_{\text{stop}}(F_i)$ is given by

$$P_{\text{stop}}(F_i) = \begin{cases} a_1(\frac{a_2L - F_i}{a_2L})^4 + \epsilon & 1 \le F_i \le a_2L \\ \epsilon & a_2L < F_i \le 0.6L, \\ Q(F_i) & 0.6L < F_i \le L \end{cases} \tag{9}$$

where $Q(F_i)$ is a fixed quadratic function approximating the tail of the family of bowl-shape functions as shown in Fig. 2. We also use the obvious terminal condition $P_{\text{stop}}(L) = 1$.

In this paper, we further approximate the values of a_1, a_2 and ϵ as functions of r, e and θ. Based on the simulation results (part of the results have been shown in [15] and [27]), a good approximation of a_1, a_2 and ϵ can be

$$a_1 = 0.4 - 0.25\lfloor r \rfloor_{0.5} - [e]_{0.1}^{0.5}(0.2 - [e]_{0.1}^{0.5}) - 0.25\lceil \theta \rceil^{0.4}, \tag{10}$$

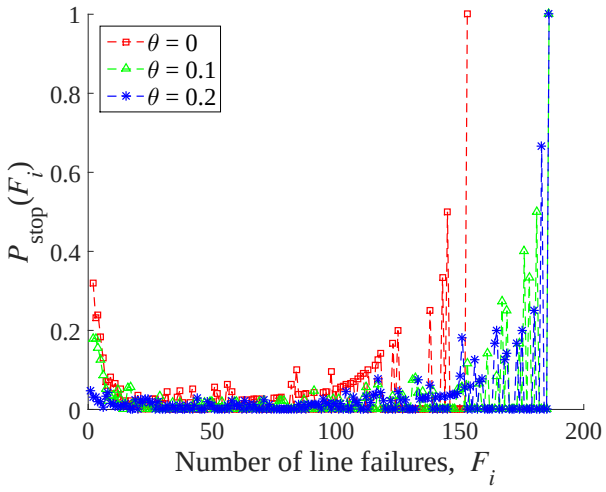

Fig. 2. The cascade-stop probability $P_{\text{stop}}(F_i)$ as estimated from simulation results. (Figure is adopted from [15].)

$$a_2 = 0.1 - 0.05\lfloor r \rfloor_{0.5} - 0.1[e]_{0.1}^{0.5}(0.2 - [e]_{0.1}^{0.5}) - 0.07\lceil \theta \rceil^{0.4}, \tag{11}$$

$$\text{and} \quad \epsilon = 0.6 - 0.4\lfloor r \rfloor_{0.5} - 0.5[e]_{0.1}^{0.5} - 0.3\lceil \theta \rceil^{0.4}. \tag{12}$$

It is noted that the values of r, e and θ are truncated in (10), (11) and (12). The reasons are twofold. On one hand, the impact of an operating characteristic on cascading failures (namely $P_{\text{stop}}(F_i)$) behaves similarly beyond certain threshold, e.g., $r < 0.5$ and $e < 0.1$, based on power-system simulation results. On the other hand, it is practical to assume that e should be less than 0.3 and θ should be less than 0.4. For convenience, we also show the analytic characterizations of a_1 and a_2 as a function of r, e and θ in Fig. 3. With the parametric modeling of $P_{\text{stop}}(F_i)$ at hand, the description of transition probabilities in the hSASE model becomes complete.

V. Blackout-Size Probability Distribution

A. Criticality Analysis Using the hSASE Model

An important consequence of the hSASE model is that it allows us to evaluate the probability mass function (PMF) of the blackout size of a cascading-failure caused by any disturbance event. Such PMF is a widely adopted metric for assessing the risk of cascading failures in the power grid.

Let $\mathcal{S}$ denote the state space of the Markov chain in the hSASE model. The total number of states in $\mathcal{S}$ is $2L|H|$ due to the definition of a state $S_i \in \mathcal{S}$ given in Section IV-B. Here L is the number of transmission lines in the power grid and $|H|$ is the cardinality of H (recall that H is the set containing all the levels of OR). Note that $|H|$ is a fixed number in the hSASE model, e.g., $|H| = 4$ for the IEEE 118-bus system studied in this paper. Hence, the size of the state space of the Markov chain scales linearly as a function of the number of transmission lines in the power system.

For convenience, the indices of all the states in the Markov chain are arranged by following three simple rules.
For any two distinct states S_i and S_j,
(i) $i < j$ if $F_i < F_j$;
(ii) $i < j$ if $F_i = F_j$ but $H_i < H_j$;

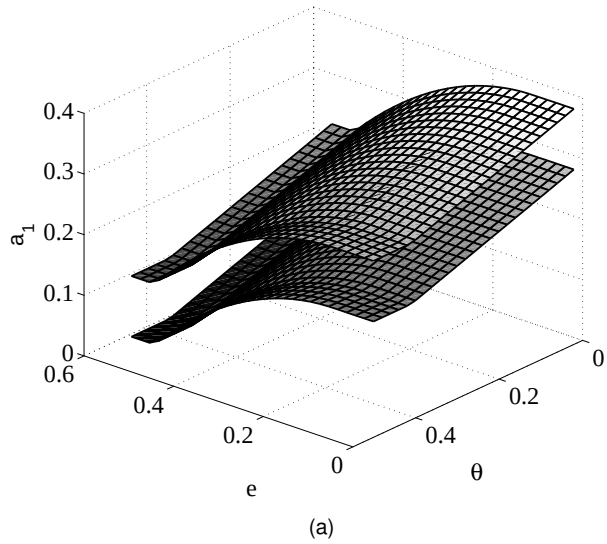

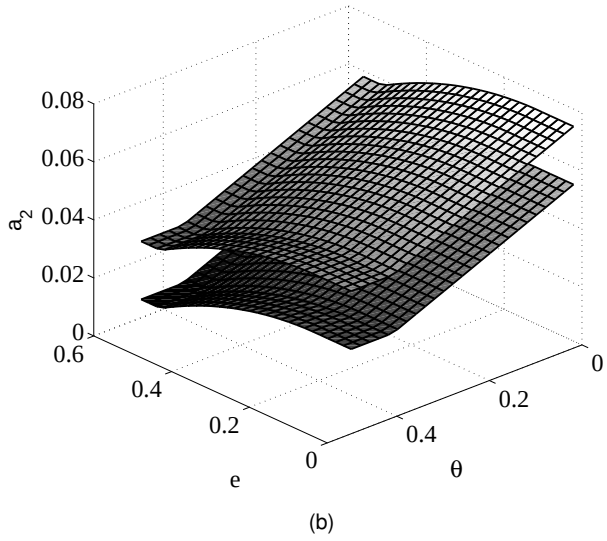

Fig. 3. Analytic characterizations of (a) a_1 and (b) a_2 as a function of r, e and θ. Upper surfaces: $r = 0.5$; lower surfaces: $r = 0.9$.

(iii) $j = i + 1$ if $F_i = F_j$ and $H_i = H_j$, but $I_i = 0$ and $I_j = 1$.
To this end, the index of a state $S_i = (F_i, H_i, I_i)$ is

$$(F_i - 1)|H| + 2(H_i - 1) + I_i + 1. \tag{13}$$

From (13), it is clear that the indices of transitory states and absorbing states are odd and even, respectively. Furthermore, if a transition from S_i to S_j has a positive probability, then the index of S_j is always larger than the index of S_i.

Now let $\boldsymbol{Q}$ be the transition matrix of the Markov chain, and q_{ij} represent the ijth element of $\boldsymbol{Q}$, i.e., $q_{ij} = P(S_j|S_i)$. It is clear that $\boldsymbol{Q}$ is a $2L|H| \times 2L|H|$ square matrix. Furthermore, two important properties of $\boldsymbol{Q}$ are given by the following two propositions and a lemma.

Proposition 1. $\boldsymbol{Q}$ is an upper diagonal matrix.

Proof. This is due to the fact that the number of failed transmission lines accumulate during cascading failures and there

is no transmission-line restoration during cascading failures in the hSASE model. □

Proposition 2. The elements on the main diagonal of $\boldsymbol{Q}$ are given by

$$q_{ii} = \begin{cases} 0 & \text{if } i \text{ is odd,} \\ 1 & \text{if } i \text{ is even.} \end{cases}$$

Proof. This is due to the definitions of a transitory state and an absorbing state given in Section IV-B. More specifically, the cascading failure proceeds when it is in a transitory state S_i (when i is odd), which implies that $q_{ii} = 0$. While the cascading failure terminates when it is in an absorbing state S_i (when i is even), which implies that $q_{ii} = 1$ and $q_{ij} = 0$ for $i \neq j$. □

Lemma 1. $\boldsymbol{Q}$ is a stochastic matrix.

Proof. We must show that $\sum_{j \in S} q_{ij} = 1$, for all $i \in S$. When i is even, it is clear from Proposition 2 that $q_{ii} = 1$ and $q_{ij} = 0$ for $i \neq j$, which implies $\sum_{j \in S} q_{ij} = 1$. When i is odd, a state $S_i = (F_i, H_i, 0)$ is a transitory state. According to the definition of transition probabilities given in equation (4), the cascade-stop transition from S_i to S_j is unique, where $j = i+1$, with $q_{ij} = P_{\text{stop}}(F_i)g(H_i)$. On the other hand, there may be multiple cascade-continue transitions from S_i to S_j for $j \in J$, where J is the set containing odd numbers in the range $[i + 2|H|, 2(F_i + 1)|H| - 1]$. Furthermore, $\sum_{j \in J} q_{ij} = 1 - P_{\text{stop}}(F_i)g(H_i)$ and $q_{ij} = 0$ for all $j \notin J$ and $j \in S$. Hence, $\sum_{j \in S} q_{ij} = 1$ when i is odd. □

Theorem 1: Starting from any initial state S_0, the state always reaches an absorbing state in the Markov chain given the transition matrix $\boldsymbol{Q}$.

Proof. It is noted that a state S_i is either transitory or absorbing. For a transitory state S_i, it can only transition to S_j with $F_j = F_i + 1$. Furthermore, if a transitory state S_i with $F_i = L - 1$ transition to the next state S_j then S_j has $F_j = L$. As the terminal condition, S_j is always an absorbing state. Theorem 1 is then established since only finite number of states will be considered in the hSASE model. □

In light of Theorem 1, we can claim that the Markov chain has a limiting distribution of states given an initial state S_0. Let the vector $\boldsymbol{\pi_0} = (0, ..., 0, 1, 0, ...0)$ denote the initial state S_0, where the position of the element that equals to "1" in $\boldsymbol{\pi_0}$ is the index of S_0 in the Markov chain. Next, let the vector $\boldsymbol{\pi} = (\pi_i, i = 1, \ldots, 2L|H|)$ represent the limiting distribution given $\boldsymbol{\pi_0}$, where π_i is the steady-state probability of S_i. Then

$$\boldsymbol{\pi} \triangleq \boldsymbol{\pi_0} \lim_{k \to \infty} \boldsymbol{Q}^k. \tag{14}$$

Now let $B(n|S_0)$ represent the summation of the steady-state probabilities of a set of states S_i with $F_i = n$. We can write

$$B(n|S_0) = \sum_{i=1}^{|H|} \pi_{2(n-1)|H|+2i}, \text{for } n = 1, \ldots, L. \tag{15}$$

It is important to note that $B(n|S_0)$ represents the probability of a blackout with n transmission-line failures given an initial disturbance S_0 in the physical sense.

It is noted that the Markov chain studied in the hSASE model is not irreducible because there exist both transient states and recurrent states in the Markov chain. This further implies that the unique stationary distribution of the Markov chain does not exist (it is not difficult to see this point since the stationary distribution is dependent on the initial state). To obtain the PMF of the blackout size (i.e., $B(n|S_0)$ for $n = 1, \ldots, L$), we can conduct Monte-Carlo simulations of the Markov chain given the initial state S_0. In this case, the computational complexity of the hSASE model scales linearly in terms of L. Alternatively, we can further obtain the analytic expression for $B(n|S_0)$ by evaluating $\lim_{k \to \infty} \boldsymbol{Q}^k$. This can be done by performing matrix diagonalization as well as using the Cayley-Hamilton theorem. For further discussion on the details of this analysis, we refer interested readers to [15].

B. Critical Operating Characteristics of the Power Grid

From the analysis of historical blackout data of the North American electric power transmission system [10], [24], [31] as well as power-system simulation results [15], [26], [27], researchers have agreed that today's power grids may be operated close to a critical setting. A widely accepted indicator of such critical setting is that the PMF of the blackout sizes does not decrease exponentially with the size of the blackout, but rather a power-law tail [32]. Hence, in this paper we define a power grid to be operating in a critical setting if the PMF of the blackout size has a power-law tail.

Given the operating characteristics of the power grid as well as the initial disturbance event S_0, we are able to obtain the PMF of blackout size of a cascading failure (namely $B(n|S_0)$) by applying the limit approach as discussed in Section V-A. The PMF of blackout size can be used to further characterize the critical operating characteristics of the power grid. In this section, we start by investigating various cascading-failure scenarios and calculate the associated PMFs of blackout size to find out how the human behavior and the three power-grid operating characteristics influence the cascading-failure behavior in the IEEE 118-bus system. Then we proceed to identify the critical operating characteristics of the power grid, which should be avoided to reduce the risk of large cascading failures. The initial disturbance event considered here is two transmission-line failures with $C^{\max}$ = 80MW.

In Fig. 4 we show the PMFs of blackout size for three different scenarios when e = 0.3 and θ = 0.3. First, it is interesting to compare the results for the two scenarios when r = 0.75. It is clear that the PMF of blackout size changes from an exponential behavior, when the human error is not considered, to a power-law tail when the human error is considered. It is also worth noting that the coupling of human behavior is not the exclusive factor that determines the criticality of the cascading failure. For example in the case when $r = 0.9$ and the human coupling is not taken into account, the PMF of blackout size also exhibits a power-law tail.

To further investigate how the cascading failure is influenced by the power-grid operating setting and the human behavior, we show another set of PMFs of blackout size in Fig. 5 for cases when e = 0.1, θ = 0.01 and the impact of human behavior has been considered. Under such a setting of e and θ, the power grid is less vulnerable to cascading failures. Hence, we observe from Fig. 5 that, as expected, all the PMFs of the blackout size approximate the exponential behavior no matter what the load ratio r is.

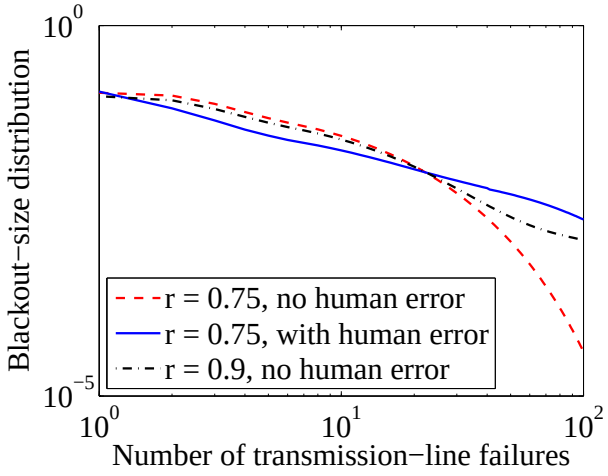

Fig. 4. The PMF of blackout size for three different scenarios: e = 0.3 and θ = 0.3.

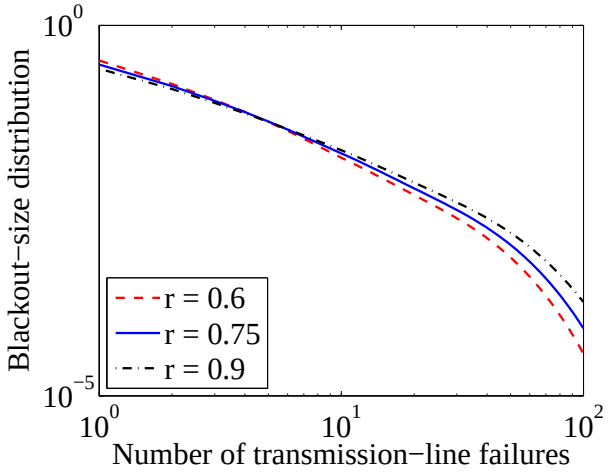

Fig. 5. The PMF of blackout size for three different loading level r when human error is considered for all scenarios: e = 0.1, θ = 0.01.

The results in Fig. 4 and Fig. 5 confirm that there exist certain critical settings (i.e., combinations of values of r, e and θ) that determine the criticality of cascading failure in the power grid. In other words, these critical points make the system sensitive to large cascading failures with the blackout probability following a power-law distribution.

In light of the proposed analytic model, we can further identify the non-critical settings for cascading failures in the power grid without running the power-system simulator, which is time consuming. In Fig. 6, two non-critical regions are shown for cases when the impact of human behavior is not considered and considered, respectively. In particular, each point inside the regions represents a specific operating setting (a combination of r, e and θ). The PMF of the blackout size under any non-critical operating setting tends to have the exponential-tail behavior rather than the power-law tail. By comparing Fig. 6(a) and Fig. 6(b), it is clear that the non-critical regions shrink due to the consideration of human error. One more important fact learned from Fig. 6 is that the impact of human error can also be illustrated as the drop of θ in the non-critical region when r and e are fixed. The observation directly implies that the power grid can enhance its tolerance to cascading failures when more load-shedding is allowed.

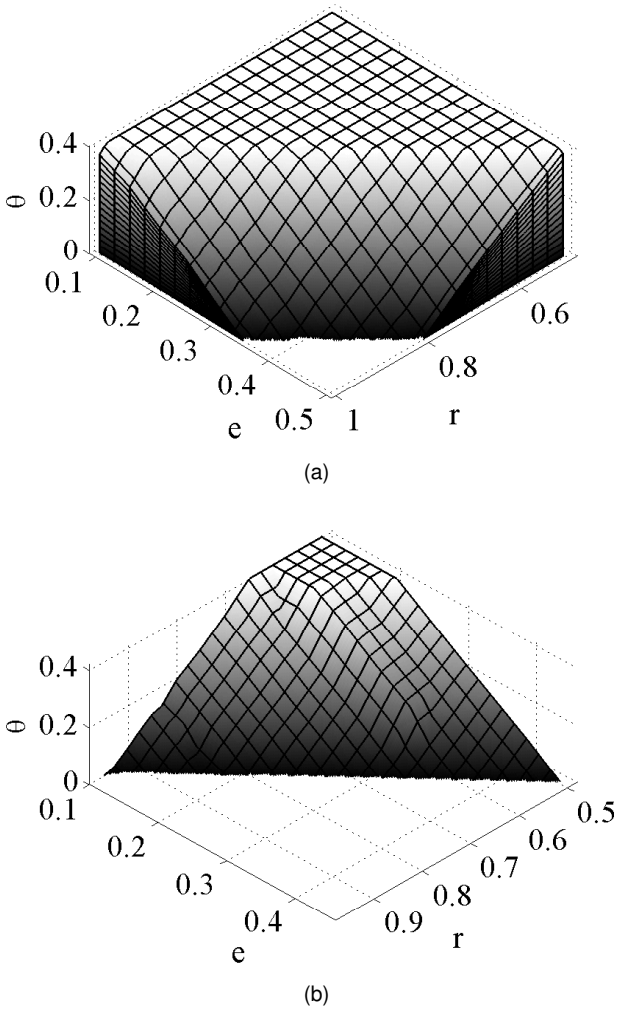

Fig. 6. Non-critical region for power-grid operating characteristics when (a) the impact of human behavior is not considered, and (b) the impact of human behavior is considered.

VI. Conclusions and Extensions

Human operators play a key role in the reliable operation of power grids. However, human operators may behave far from optimum. The reasons may include stressful situations and other factors that affect the reliability of power grids. Historical blackout data as well as interviews of power-system operators illustrate that human behavior can highly impact cascading failures in power grids. To quantify the human error during cascading failures, the SPAR-H methodology is used to estimate the HEP for the human failure events in terms of probabilistic risk assessment.

With the assessment of HEP at hand, we have developed a scalable analytic model, based upon reduced state-space Markov chains, to investigate the cascading failures in power grids when human behavior is considered. With the help of power-system simulations, we have further formulated the

state-dependent transition probabilities in the Markov chain in terms of the HEP as well as three key power-system operating characteristics including the power-grid loading level, line tripping threshold, and load-shedding constraint level. In light of the proposed analytic model, the criticality of key power-system operating characteristics can be identified. In particular, non-critical regions of the three operating-characteristic settings have been suggested, under which the power grid may become less vulnerable to severe cascading failures (the PMF of blackout size due to cascading failures decreases exponentially rather than having a power-law tail). The results can provide invaluable design and management for power-system robustness as a contribution to operate smart grids as well as a model to analyze the impact of human factors on cascading failures.

As a starting point of this work, we have only focused on the number of transmission-line failures and the loss of transmission capacity. However, the proposed analytic framework is capable of tracking other types of failures and investigating the impact of other physical attributes in the power system, such as generators, on cascading failures. For example, we can extend the definition of the state space (e.g., by introducing a state variable G_i representing the number of generator failures) of the Markov chain to track other variables in the system. Introducing new state variables (e.g., number of generator failures) also mandates generating supporting simulations to be able to estimate and relate the transition probabilities of the Markov chain to all the state variables.

REFERENCES

[1] G. Andersson *et al.*, "Causes of the 2003 major grid blackouts in north america and europe, and recommended means to improve system dynamic performance," *IEEE Transactions on Power Systems,*, vol. 20, no. 4, Nov. 2005.

[2] "Arizona-southern california outages on september 8, 2011: Causes and recommendations," FERC and NERC, Tech. Rep., April 2012. [Online]. Available: https://www.ferc.gov

[3] P. Pourbeik, P. S. Kundur, and C. W. Taylor, "The anatomy of a power grid blackout," *IEEE Power and Energy Magazine*, vol. 4, no. 5, pp. 22–29, 2006.

[4] M. Amin, "Challenges in reliability, security, efficiency, and resilience of energy infrastructure: Toward smart self-healing electric power grid," in *Power and Energy Society General Meeting-Conversion and Delivery of Electrical Energy in the 21st Century*. IEEE, 2008, pp. 1–5.

[5] J. Park *et al.*, "Analysis of operators' performance under emergencies using a training simulator of the nuclear power plant," *Reliability Engineering & System Safety*, vol. 83, no. 2, pp. 179–186, 2004.

[6] C. R. Lawton and J. H. Gauthier, "Human performance modeling in system of systems analytics," in *System of Systems Engineering (SoSE), 2012 7th International Conference on*. IEEE, 2012, pp. 77–82.

[7] J. M. Abreu *et al.*, "Modeling human reliability in the power grid environment: an application of the spar-h methodology," in *Proceedings of the Human Factors and Ergonomics Society Annual Meeting*, vol. 59, no. 1. SAGE Publications, 2015, pp. 662–666.

[8] M. Panteli and D. S. Kirschen, "Situation awareness in power systems: Theory, challenges and applications," *Electric Power Systems Research*, vol. 122, pp. 140–151, 2015.

[9] M. Bessani *et al.*, "Impact of operators performance in the reliability of cyber-physical power distribution systems," *IET Generation, Transmission & Distribution*, vol. 10, no. 11, pp. 2640–2646, 2016.

[10] B. A. Carreras, V. E. Lynch, I. Dobson, and D. E. Newman, "Complex dynamics of blackouts in power transmission systems," *Chaos: An Interdisciplinary Journal of Nonlinear Science*, vol. 14, no. 3, pp. 643–652, 2004.

[11] J. Chen, J. S. Thorp, and I. Dobson, "Cascading dynamics and mitigation assessment in power system disturbances via a hidden failure model," *International Journal of Electrical Power & Energy Systems*, vol. 27, no. 4, pp. 318–326, 2005.

[12] I. Dobson, B. A. Carreras, and D. E. Newman, "A loading-dependent model of probabilistic cascading failure," *Probability in the Engineering and Informational Sciences*, vol. 19, no. 01, pp. 15–32, 2005.

[13] M. Anghel, K. A. Werley, and A. E. Motter, "Stochastic model for power grid dynamics," in *40th Annual Hawaii International Conference on System Sciences, HICSS 2007*, pp. 113–113.

[14] M. Rahnamay-Naeini, Z. Wang, A. Mammoli, and M. M. Hayat, "A probabilistic model for the dynamics of cascading failures and blackouts in power grids," in *2012 Power and Energy Society General Meeting*, 2012, pp. 1859–1864.

[15] M. Rahnamay-Naeini, Z. Wang, N. Ghani, A. Mammoli, and M. M. Hayat, "Stochastic analysis of cascading-failure dynamics in power grids," *IEEE Transactions on Power Systems*, vol. 29, no. 4, pp. 1767–1779, 2014.

[16] J. Song, E. Cotilla-Sanchez, G. Ghanavati, and P. D. Hines, "Dynamic modeling of cascading failure in power systems," *IEEE Transactions on Power Systems*, vol. 31, no. 3, pp. 2085–2095, 2016.

[17] J. Bialek, E. Ciapessoni, D. Cirio, E. Cotilla-Sanchez, C. Dent, I. Dobson, P. Henneaux, P. Hines, J. Jardim, S. Miller *et al.*, "Benchmarking and validation of cascading failure analysis tools," *IEEE Transactions on Power Systems*, vol. 31, no. 6, pp. 4887–4900, 2016.

[18] X. Zhang, C. Zhan, and K. T. Chi, "Modeling the dynamics of cascading failures in power systems," *IEEE Journal on Emerging and Selected Topics in Circuits and Systems*, 2017.

[19] D. Gertman, H. Blackman, J. Marble, J. Byers, C. Smith *et al.*, "The spar-h human reliability analysis method," *US Nuclear Regulatory Commission*, 2005.

[20] M. Azadeh, A. Keramati, I. Mohammadfam, and B. Jamshidnedjad, "Enhancing the availability and reliability of power plants through macroergonomics approach," *Journal of Scientific and Industrial research*, vol. 65, no. 11, p. 873, 2006.

[21] H. S. Blackman, D. I. Gertman, and R. L. Boring, "Human error quantification using performance shaping factors in the spar-h method," in *Proceedings of the Human Factors and Ergonomics Society Annual Meeting*, vol. 52, no. 21. SAGE Publications, 2008, pp. 1733–1737.

[22] R. L. Boring and H. S. Blackman, "The origins of the spar-h methods performance shaping factor multipliers," in *2007 IEEE 8th Human Factors and Power Plants and HPRCT 13th Annual Meeting*, pp. 177–184.

[23] R. Moura, M. Beer, E. Patelli, J. Lewis, and F. Knoll, "Learning from major accidents to improve system design," *Safety science*, vol. 84, pp. 37–45, 2016.

[24] B. A. Carreras, V. E. Lynch, I. Dobson, and D. E. Newman, "Critical points and transitions in an electric power transmission model for cascading failure blackouts," *Chaos: An interdisciplinary journal of nonlinear science*, vol. 12, no. 4, pp. 985–994, 2002.

[25] D. S. Kirschen, D. Jayaweera, D. P. Nedic, and R. N. Allan, "A probabilistic indicator of system stress," *IEEE Transactions on Power Systems*, vol. 19, no. 3, pp. 1650–1657, 2004.

[26] D. P. Nedic, I. Dobson, D. S. Kirschen, B. A. Carreras, and V. E. Lynch, "Criticality in a cascading failure blackout model," *International Journal of Electrical Power & Energy Systems*, vol. 28, no. 9, pp. 627–633, 2006.

[27] M. Rahnamay-Naeini and M. M. Hayat, "Impacts of operating characteristics on sensitivity of power grids to cascading failures," in *2016 Power and Energy Society General Meeting*, 2016.

[28] B. Liscouski and W. Elliot, "Final report on the august 14, 2003 blackout in the united states and canada: Causes and recommendations," *A report to US Department of Energy*, vol. 40, no. 4, 2004.

[29] R. D. Zimmerman, C. E. Murillo-Sánchez, and R. J. Thomas, "Matpower: Steady-state operations, planning, and analysis tools for power systems research and education," *IEEE Transactions on power systems*, vol. 26, no. 1, pp. 12–19, 2011.

[30] Q. Chen and L. Mili, "Composite power system vulnerability evaluation to cascading failures using importance sampling and antithetic variates," *IEEE Transactions on Power Systems*, vol. 28, no. 3, pp. 2321–2330, 2013.

[31] B. A. Carreras, D. E. Newman, I. Dobson, and A. B. Poole, "Evidence for self-organized criticality in a time series of electric power system blackouts," *IEEE Transactions on Circuits and Systems I: Regular Papers*, vol. 51, no. 9, pp. 1733–1740, 2004.

[32] I. Dobson, B. A. Carreras, V. E. Lynch, and D. E. Newman, "An initial model for complex dynamics in electric power system blackouts," in *34th Hawaii International Conference on System Sciences*, Jan. 2002.

Zhuoyao Wang received the B.Eng. degree from Jilin University, Jilin, China, in 2008, and the M.S. and Ph.D. degrees in electrical and computer engineering from the University of New Mexico, Albuquerque, NM, USA, in 2011 and 2016, respectively. From June 2016 to September 2017, he served as a Post-doctoral Fellow in the Center for High Technology Materials at the University of New Mexico. He is currently a software engineer at Tencent, Shenzhen, China. His research interests include analysis of cascading failures in smart grids, resource provisioning in the cloud and load balancing in distributed systems.

Mahshid Rahnamay-Naeini received the B.Sc. degree in computer engineering from the Sharif University of Technology in 2007, the M.Sc. degree in computer networks from the Amirkabir University of Technology in 2009, and the Ph.D. degree in electrical and computer engineering with a minor in mathematics from the University of New Mexico in 2014. She is an Assistant Professor with the Electrical Engineering Department at The University of South Florida. Her research interest lies in the areas of Network Science, Stochastic Processes, System Modeling, Network Analytics, Machine Learning, and Prediction Models with applications in Communication Networks, Software Defined Networking, Cyber-Physical-Human Systems with particular emphasis on Smart Grids, and their Reliability, Security and Performance Evaluation.

Joana Abreu received her Ph.D. degree in sustainable energy systems from the MIT Portugal, Instituto Superior Técnico, Massachusetts Institute of Technology, in 2012. She leads behavioral research for Fraunhofer CSEs Building Energy Management Group. At Fraunhofer CSE, she works with a team comprising engineers, building scientists and psychologists to apply experimental psychology methods to complex systems-level research in both field and laboratory research projects. She developed an externally-funded interdisciplinary research program that includes such diverse subjects as energy efficiency, social science, data analytics, environmental engineering and geographical information systems.

Rezoan A. Shuvro received his B.Eng. degree from Khulna University of Eng. & Tech, Bangladesh, in 2010. He worked for almost six years in one of the leading telecom operators in the world (Telenor group) as an RF Planning and Optimization Engineer. He is currently working towards the Ph.D. degree in electrical and computer engineering department at the University of New Mexico, Albuquerque, NM, USA. His research is focused on performance modeling, cascading failures in interdependent systems, reliability and performance analysis of communication networks using Markov chains.

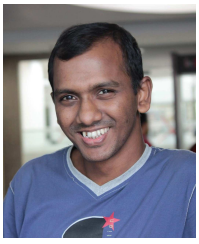

Pankaz Das received his B.Sc. in Electronics and Communication Engineering from Khulna University of Engineering and Technology, Bangladesh in 2010. He completed his M.Sc. in Electronics Engineering from Kookmin University, South Korea in 2013. After that, he worked in Samsung R&D Institute as a Senior Software Engineer for two years. Currently he has been working towards his Ph.D. degree, where his research is focused on reliability and resiliency analysis of heterogeneous coupled multi-layer systems, including power systems, communication networks and human factors.

Andrea A. Mammoli received the B.Eng. and Ph.D. degrees from the Department of Mechanical and Materials Engineering, University of Western Australia, Crawley, Australia. He is a Professor of mechanical engineering and Director of the University of New Mexico (UNM) School of Engineerings Center for Emerging Energy Technologies, Albuquerque, NM, USA. He also holds a secondary appointment with the Department of Electrical and Computer Engineering at UNM. After two years as a Director-funded Postdoctoral Fellow with Los Alamos National Laboratory, in 1997, he joined the UNM as a Research Assistant Professor. Until 2004, he conducted research in the flow of heterogeneous materials, using both experimental techniques (nuclear magnetic resonance, particle image velocimetry and rheometry) as well as high-performance direct numerical simulation using primarily boundary element techniques. Stimulated by a DOE-sponsored project on CO2 sequestration, and by a sabbatical year at the Universit Politecnica delle Marche in Italy, in 2005, he steered his research activities to the area of energy systems, beginning with a project to refurbish and modernize the solar-assisted HVAC in the UNM Mechanical Engineering building. He collaborates with the utility industry and national laboratories (Sandia, Berkeley and Los Alamos) on various demonstration projects and testbeds to bring new technologies online speedily.

Nasir Ghani received his Ph.D. in computer engineering from the University of Waterloo, Canada, in 1997. He is a Professor of Electrical Engineering at the University of South Florida (USF) and Research Liaison for the Florida Center for Cybersecurity (FC2). Earlier he was Associate Chair of the ECE Department at the University of New Mexico (2007-2013) and a faculty member at Tennessee Tech University (2003-2007). He also spent several years working in industry at large Blue Chip organizations (IBM, Motorola, Nokia) and hi-tech startups. His research interests include cyberinfrastructure networks, cybersecurity, cloud computing, disaster recovery, and cyber-physical systems. He has published over 200 peer-reviewed articles and has several highly-cited US patents. He is an Associate Editor for IEEE/OSA Journal of Optical and Communications and Networking and has served as an editor for IEEE Systems and IEEE Communications Letters. He has also guest-edited special issues of IEEE Network and IEEE Communications Magazine and has chaired symposia for numerous IEEE conferences. Dr. Ghani also chaired the IEEE Technical Committee on High Speed Networking (TCHSN) from 2007-2010.

Majeed M. Hayat received a BS degree (summa cum laude) in electrical engineering from the University of the Pacific, Stockton, CA, in 1985. He received the MS and the PhD degrees in electrical and computer engineering from the University of Wisconsin-Madison in 1988 and 1992, respectively. He is currently a Professor of electrical and computer engineering at the University of New Mexico in Albuquerque, NM, USA. His research activities cover a broad range of topics including networked computing, interdependent networks and systems with applications to smart grids, avalanche photodiodes, high-speed optical communication, signal processing for synthetic aperture radar, and compressive algorithms for spectral sensing and imaging. Dr. Hayat was Associate Editor of Optics Express from 2004 to 2009, Chair of the Topical Subcommittee of the IEEE Photonics Society from 2009 to 2013. He is currently Associate Editor of the IEEE Transactions on Parallel and Distributed Systems. He is recipient of the NSF Early Faculty Career Award (1998). He has authored over 100 journal articles, with nearly 4,500 citations and an h-Index of 33. He has 12 issued patents, four of which have been licensed. Dr. Hayat is a fellow of IEEE, SPIE and OSA.